Control of the Rate of the Electrochemical Oxidation of the Dimeric Aquomolybdenum(III) Cation by the Rate of Its Deprotonation

Sir:

The electrochemical intraconversion of the dimeric Mo^{V}_2 and Mo^{III}_2 aquo ions is highly asymmetric.[1] The reduction and reoxidation reactions proceed at very different potentials, and the oxidation of Mo^{III}_2 becomes independent of potential while its rate is well below the diffusion-limited value. In a previous study[1] these facts were attributed to the large structural differences that were expected to distinguish Mo^{III}_2 and Mo^{V}_2 aquo ions. Recently, EXAFS experiments[2] have suggested possible structures for the two ions that require extensive deprotonation to accompany the oxidation of Mo^{III}_2. In this study we have attempted to discern such structural changes by examining the electrode kinetics and measuring the corresponding proton reaction orders for both of the dimeric aquo ions. The electrochemical results are consistent with the structural differences between the two ions proposed on the basis of the EXAFS study.

Experimental Section. Materials. Most reagents, including sodium molybdate, were reagent grade and were used as received. Trifluoromethanesulfonic acid was purified by distillation as previously described.[1] Solutions of $Mo_2O_4^{2+}$ were prepared by electrolytic reduction of molybdate solutions[1] or by chemical reduction with hydrazine followed by purification via cation exchange on Bio-Rad AG 50W-X2 resin. The molar extinction of $Mo_2O_4^{2+}$ at 296 nm was measured as 3.21×10^3 M^{-1} cm^{-1} in 2 M trifluoromethanesulfonic acid.[3] This value is similar to a value reported[4] in 1 M perchloric acid (3.37×10^3 M^{-1} cm^{-1}).

Apparatus and Procedures. Instrumentation employed to carry out electrochemical and spectroscopic measurements has been described previously.[5] Dropping-mercury or hanging-mercury-drop electrodes were utilized. The mercury flow rate of the DME was 0.9–1.2 mg s^{-1}. The area of the HMDE was 0.032 cm^2. Experiments were conducted at the ambient laboratory temperature (22 ± 2 °C) in solutions that were deaerated with prepurified argon. Potentials were measured and are reported with respect to a saturated calomel reference electrode (SCE).

Results. Cyclic and Staircase Voltammetry of $Mo_2O_4^{2+}$. The cyclic voltammetry of $Mo_2O_4^{2+}$ in 2 M trifluoromethanesulfonic acid has been described.[1] The diffusion-controlled, four-electron wave for the reduction of Mo^{V}_2 is widely separated from that for the reoxidation of Mo^{III}_2. The latter process is also not diffusion controlled. A slow chemical step intervenes to prevent the appearance of a clear current peak and to depress the oxidation current to values well below those obtained for the reduction of Mo^{V}_2. However, exhaustive electrolyses show that the electrooxidation of Mo^{III}_2 leads only to Mo^{V}_2[1,3] so that the smaller oxidation currents do not reflect differences in the reaction stoichiometry between reduction and oxidation steps. These features are evident in the typical cyclic voltammograms shown in Figure 1A.

Decreasing the acidity at constant ionic strength produces some changes in the cyclic voltammetric responses as shown in Figure 1B. Both the reduction and oxidation waves shift to more negative potentials, the anodic peak current, while still less than that for the reduction of Mo^{V}_2, becomes relatively larger, and the wave shape is more peaked. The cathodic peak current is diffusion controlled at scan rates of 50 mV s^{-1} or higher (inset in Figure 1B), but a lower scan rates the currents are anomalously large and the wave is misshapen. This

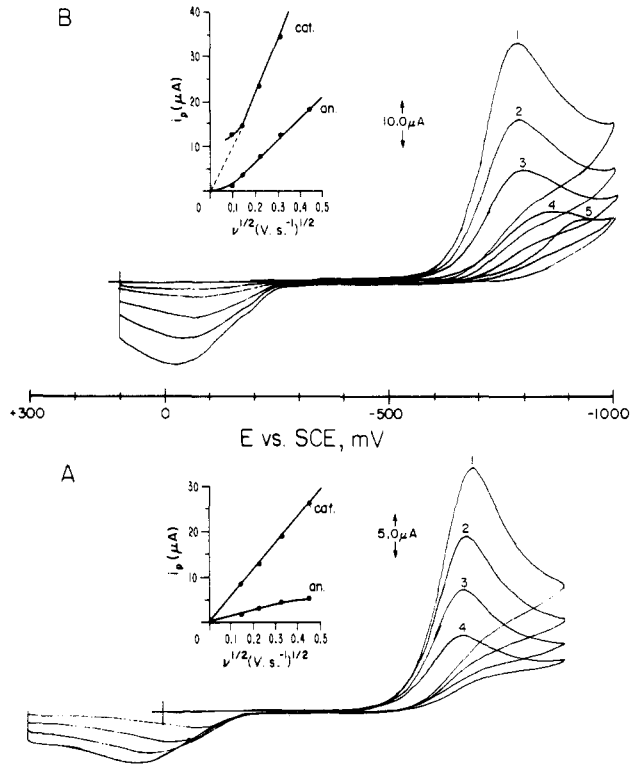

Figure 1. Representative cyclic voltammetry of Mo^{V}_2: (A) 0.56 mM Mo^{V}_2 in 2.0 M trifluoromethanesulfonic acid; (B) 1.1 mM Mo^{V}_2 in 0.2 M trifluoromethanesulfonic acid + 1.8 M lithium trifluoromethanesulfonate. Scan rates (mV s^{-1}): (1) 200; (2) 100; (3) 50; (4) 20; (5) 10. The potential axis applies to both sets of curves. Insets show peak current vs. (scan rate)$^{1/2}$ for the reduction (cat.) and oxidation (an.) peaks.

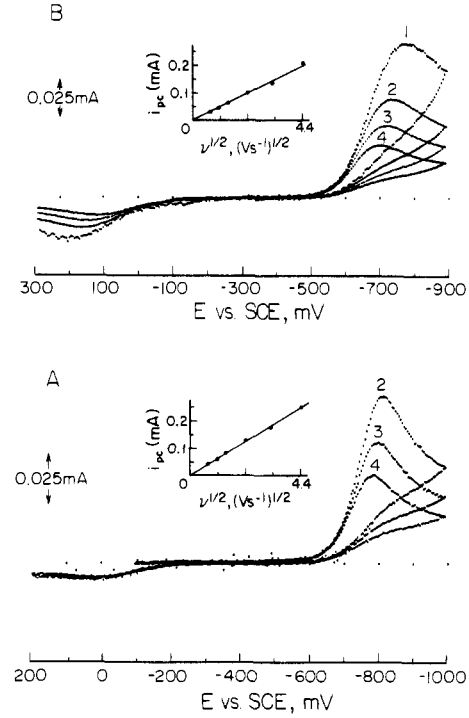

Figure 2. Cyclic staircase voltammograms for Mo^{V}_2: (A) 1.0 mM Mo^{V}_2; (B) 1.1 mM Mo^{V}_2. Potential step height: 4.88 mV. Effective scan rates (adjusted by changing the pulse widths; V s^{-1}): (1) 5; (2) 2; (3) 1; (4) 0.5. Supporting electrolytes are as in Figure 1.

(1) Chalilpoyil, P.; Anson, F. C. *Inorg. Chem.* **1978**, *17*, 2418.
(2) Cramer, S.; Eidem, P.; Paffett, M.; Winkler, J.; Dori, Z.; Gray, H. B. *J. Am. Chem. Soc.* **1983**, *105*, 799.
(3) Paffett, M. T. Ph.D. Thesis, California Institute of Technology, 1983.
(4) Armstrong, F. A.; Sykes, A. G. *Polyhedron* **1982**, *1*, 109.
(5) Paffett, M. T.; Anson, F. C. *Inorg. Chem.* **1983**, *22*, 1347; **1981**, *20*, 3967.

0020-1669/84/1323-1996$01.50/0

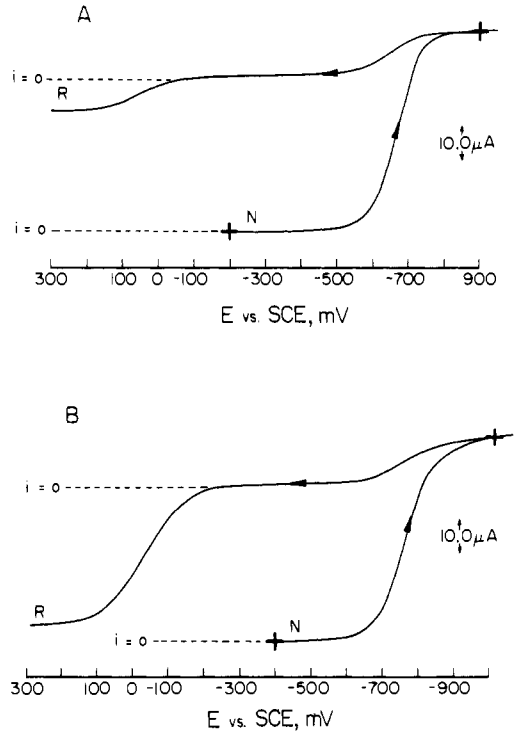

Figure 3. Normal- (N) and reverse- (R) pulse polarograms for 1.1 mM Mo^{V}_2. Supporting electrolyte: (A) 2 M trifluoromethanesulfonic acid; (B) 0.2 M trifluoromethanesulfonic acid + 1.8 M lithium trifluoromethanesulfonate. Pulse width: 18.2 ms. Drop time: 1 s.

phenomenon was not investigated further and was generally avoided by restricting measurements to situations where the anomalies were absent.

To extend the measurements to higher scan rates, staircase voltammetry was employed because of the better ratio of Faradaic to non-Faradaic current obtainable with this technique.[6] In Figure 2 a set of cyclic staircase voltammograms is shown for the same two supporting electrolyses employed in Figure 1. The cathodic peak currents remain diffusion controlled at the higher (effective) scan rates, but the peak potentials become more sensitive to the scan rate, especially with the 0.2 M acid solution. The anodic currents are essentially independent of scan rate in 2 M acid and become so in 0.2 M acid at scan rates above 5 V s^{-1} (not shown).

Pulse Polarography. To allow a quantitative assessment of the factors controlling the rates of Mo^{V}_2 reduction and Mo^{III}_2 oxidation, these reactions were examined by normal- and reverse-pulse polarography.[7] Representative polarograms at two different acidities are shown in Figure 3. As expected from the voltammetric behavior, the normal-pulse polarograms for the reduction of Mo^{V}_2 have diffusion-limited plateau currents that do not depend on the acidity of the supporting electrolyte although the half-wave potentials shift to more negative values at lower acidities. The reverse-pulse polarograms exhibit the two waves expected for redox couples in which the reduction and oxidation steps proceed at widely separated potentials. The plateau current of the first wave in the reverse-pulse polarogram appears at the same potential as the normal-pulse polarographic wave and corresponds to

Table I. Values of k_1K (s^{-1}) for the Deprotonation of Mo^{III}_2 prior to Its Oxidation to Mo^{V}_2

t_p,[a] ms	[H+],[b] M 2.0	1.0	0.4	0.2
54.9	1.53	10.0		
18.2	1.41	10.6	46.5	
10.5	0.50	9.6	46.7	186
5.05	0.97	11.4	38.3	198
	1.1[c]	10.4[c]	44[c]	192[c]

[a] Width of the normal-pulse polarographic potential step. [b] Ionic strength maintained at 2.0 M with CF_3SO_3Li. [c] Average.

Table II. Normal-Pulse Polarographic Half-Wave Potentials for the Reduction of Mo^{V}_2

[H+],[a] M	$-E_{1/2}$,[b] mV vs. SCE	[H+],[a] M	$-E_{1/2}$,[b] mV vs. SCE
2.0	645	0.2	737
1.0	670	0.48	769
0.5	693		

[a] Ionic strength maintained at 2.0 M with CF_3SO_3Li. [b] Pulse width 18.2 ms.

the Ilkovic current for the reduction of Mo^{V}_2. The magnitude of the plateau current for this wave is not affected by the acidity of the solution and agrees with the value calculated from the normal-pulse polarogram.[7] The second wave with a more positive half-wave potential results from the oxidation of Mo^{III}_2 that is generated at the electrode surface at the initial potential (−900 or −1000 mV). The magnitude of the plateau current of this anodic wave is influenced strongly by the acidity of the supporting electrolyte as well as the pulse width (i.e., the time after each potential step when the resulting current is measured). At the lowest proton concentration that could be used without overlap of the reduction wave with the background current from reduction of the supporting electrolyte (0.048 M), the total plateau current for the reverse-pulse polarogram (i.e., the sum of the plateau currents for the two waves) matched that of the normal-pulse polarogram. Under these conditions both the reduction of Mo^{V}_2 and the reoxidation of the resulting Mo^{III}_2 proceeded at diffusion-controlled rates. However, with higher proton concentrations the rate of the latter process became slower as reflected in the smaller reverse-pulse plateau currents. Under these conditions the oxidation of Mo^{III}_2 was limited by the rate of a chemical reaction that converted the complex from its predominant, unoxidizable form, $[Mo^{III}_2]^{4+}$, into an oxidizable form, $[Mo^{III}_2]^{(4-q)+}$. The net reaction rate is evidently influenced by the proton concentration (Figure 3) so that the process involved may be written in a generalized form as in reaction 1.

$$[Mo^{III}_2]^{4+} \underset{k_{-1}}{\overset{k_1}{\rightleftharpoons}} [Mo^{III}_2]^{(4-q)+} + qH^+ \qquad (1)$$

To obtain information on the kinetics of this reaction the plateau current of the second reverse-pulse wave was measured as a function of the pulse width and solution acidity. The ratios of these kinetically limited plateau currents to the diffusion-limited current obtained at the lowest proton concentration (0.048 M) are related to the kinetics of reaction 1 according to eq 2,[8] where $Z = (k_1Kt_p)^{1/2}$, $K = k_1[k_{-1}[H^+]^q]^{-1}$, t_p is the pulse width, and erfc is the complement of the error function.

$$i/i_d = \pi^{1/2}Z \exp(Z^2) \operatorname{erfc}(Z) \qquad (2)$$

(6) (a) Barker, G. C. *Adv. Polarogr., Proc. Int. Congr., 2nd* **1960**, *1*, 144. (b) Christie, H. J.; Lingane, P. J. *J. Electroanal. Chem.* **1965**, *10*, 176. (c) Mann, C. K. *Anal. Chem.* **1961**, *33*, 1484. (d) *Ibid.* **1965**, *37*, 326. (e) Zipper, J. J.; Perone, S. P. *Ibid.* **1973**, *45*, 452. (f) Ferrier, D. R.; Schroeder, R. R. *J. Electroanal. Chem. Interfacial Electrochem.* **1973**, *45*, 353. (g) Ryan, M. D. *Ibid.* **1977**, *79*, 105. (h) Miaw, H.-L.; Perone, S. P. *Anal. Chem.* **1978**, *50*, 1989.

(7) Oldham, K.; Parry, E. *Anal. Chem.* **1970**, *42*, 229. Osteryoung, J.; Kirowa-Eisner, E. *Ibid.* **1980**, *52*, 62.

(8) Bard, A. J.; Faulkner, L. R. "Electrochemical Methods"; Wiley: New York, 1980; p 444.

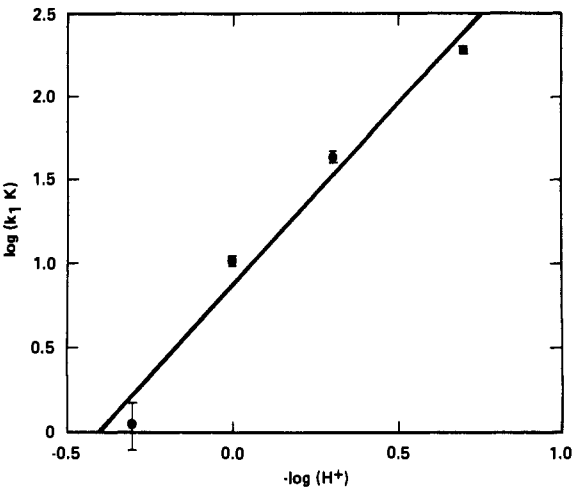

Figure 4. Average values of log (k_1K) vs. −log [H⁺] for the deprotonation of Mo^{III}_2.

Table I contains a set of data obtained at acid concentrations between 0.2 and 2 M. The values of k_1K are reasonably constant at each acid concentration as expected if the current-limiting reaction were of the type given in reaction 1. The lack of a value of the pK_a for the acid dissociation of $[Mo^{III}_2]^{4+}$ prevented us from estimating the values of the rate constants k_1 and k_{-1}. However, since eq 2 is valid only if $K \ll 1$, the reasonable constancy of the values of k_1K in Table I at $[H^+] = 1$ M indicates that k_1 is much smaller than k_{-1}.

A plot of log (k_1K) at each acidity vs. pH is shown in Figure 4. The slope of the line drawn through the points is 2.1, indicating that the value of q in reaction 1 is 2.

The half-wave potential for the reduction of Mo^V_2 shifts to more negative values with decreases in the concentration of protons (Table II). An approximate proton reaction order for the electrode reaction was obtained from the changes in the reduction currents measured at a fixed potential (−600 mV) on the foot of the polarographic waves ($i/i_d < 0.1$) as the proton concentration was changed. An estimated reaction order of 1.2 resulted. This behavior shows that the Mo^V_2 complex acquires one or more protons prior to accepting electrons. However, in contrast with Mo^{III}_2, the rates of the proton transfer reactions to Mo^V_2 are rapid enough so that they do not affect the magnitudes of the measured currents.

Discussion. The large difference between the potentials where Mo^V_2 is reduced to Mo^{III}_2 and those where the reverse process occurs is matched by significant differences in the rates of the accompanying proton-transer reactions. The acceptance of electrons by Mo^V_2 is preceded (and probably followed) by rapid protonation reactions. By contrast, the removal of electrons from Mo^{III}_2 proceeds at a rate that is limited by a prior reaction in which two protons are removed from the complex. The structure of Mo^V_2 in aqueous acid is believed to be[9]

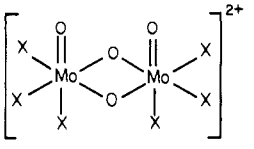

Mo^V_2, X = H_2O

For Mo^{III}_2, the combination of cation-exchange behavior, indicating a net charge of 4+,[10] and EXAFS studies,[2] ruling out the presence of a linear oxo bridging ligand, suggests the structure

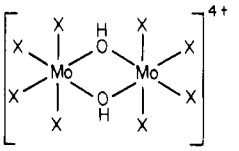

$[Mo^{III}_2]^{4+}$, X = H_2O (nonelectroactive)

The oxidation of Mo^{III}_2 to Mo^V_2 involves the loss of six protons according to these two structures. The reverse-pulse polarographic data indicate that the departure of the first two protons from Mo^{III}_2 is the slow step that limits the rate of its oxidation. A large number of possible structures can be envisioned for the deprotonated electroactive form of Mo^{III}_2. The one we prefer, shown below, places two hydroxo ligands in the sites on the molybdenum centers where the greatest structural changes occur during the course of the oxidation, namely, the sites that are occupied by the terminal oxo ligands in Mo^V_2.

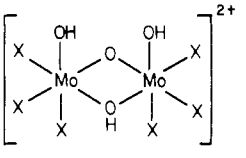

$[Mo^{III}_2]^{2+}$, X = H_2O (electroactive)

The large separation between the potentials where Mo^V_2 is reduced and Mo^{III}_2 is reoxidized is not a reflection of the kinetics of the deprotonation reactions that control the magnitude of the limiting oxidation current. Even after the preliminary deprotonation, the structures of the Mo^{III}_2 and Mo^V_2 cations evidently remain sufficiently different that a large activation barrier to electron-transfer remains. Electrooxidation of the monomeric Mo(III) aquo ion to Mo(V) (which subsequently dimerizes to Mo^V_2) also proceeds at a rate that is limited by a preceding chemical step.[1] Conversion of the aquo Mo(III) ion to the corresponding hydroxo (or oxo) complex seems likely to be the current-limiting reaction in this case as well.

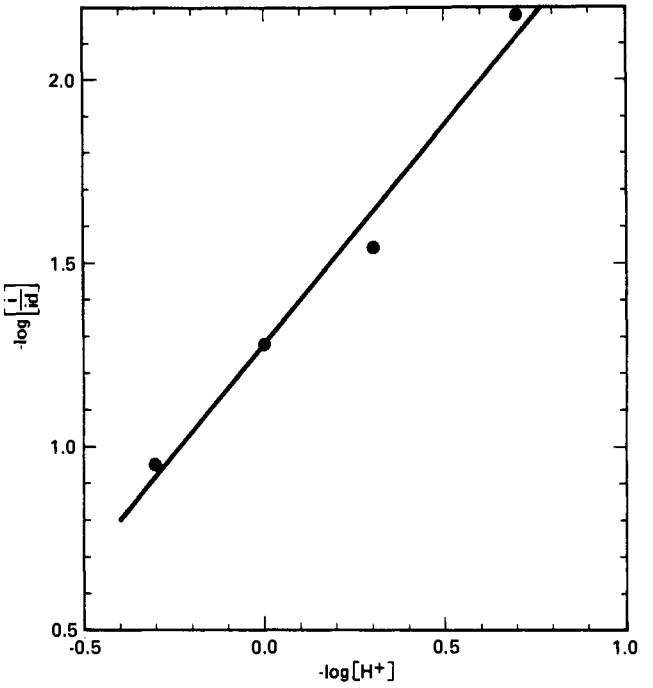

Figure 5. Proton reaction order plot for the reduction of Mo^V_2. The reduction currents were measured at −600 mV. Pulse width: 18.2 ms.

(9) Ardon, M.; Pernick, A. *J. Less-Common Met.* **1977**, *54*, 233. Cotton, F. A.; Wilkinson, G. "Advanced Inorganic Chemistry", 4th ed.; Wiley: New York, 1980; p 868.
(10) Ardon, M.; Pernick, A. *Inorg. Chem.* **1974**, *13*, 2275.

Acknowledgment. This work was supported by the National Science Foundation. Numerous helpful discussions with Dr. Jay Winkler are a pleasure to acknowledge.

(11) Contribution No. 6988.
(12) Present address: Los Alamos National Laboratory, Los Alamos, NM 87545.

Arthur Amos Noyes Laboratories[11]
Division of Chemistry and Chemical Engineering
California Institute of Technology
Pasadena, California 91125

Mark T. Paffett[12]
Fred C. Anson*

Received February 15, 1984

Generation of Metallocarboxylic Acid Anions in the Gas Phase

Sir:

We describe here the formation and reactivity of several metallocarboxylic acid anions, $M(CO)_nCOOH^-$, in the gas phase and discuss the implications of these findings for homogeneous catalysis of the water gas shift reaction (WGSR) by transition-metal carbonyls.[1-3]

As part of a larger program of study of the reactions of bare and partially solvated gas-phase ions with transition-metal compounds using the flowing afterglow method,[4] we have recently observed a remarkable effect of reactant ion hydration on the reaction between OH^- and $Fe(CO)_5$ (eq 1).[5] Bare

$$HO(H_2O)_n^- + Fe(CO)_5 \xrightarrow{n=0} Fe(CO)_3OH^- + 2CO \quad (1)$$
$$\xrightarrow{n=1-4} Fe(CO)_5OH^- + nH_2O$$

hydroxide ion and each of the cluster ions shown above all react with $Fe(CO)_5$ at or near the collision rate.[6] In the former case, a coordinatively unsaturated iron tricarbonyl hydroxide ion results by expulsion of two CO ligands[7] while the hydrated species all yield a hydroxide adduct by exclusive loss of water molecules. We find this behavior to be general for several other group 6 metal carbonyls (eq 2–4). Several analogous

$$Cr(CO)_{3,4}OH^- \xleftarrow{n=0} HO(H_2O)_n^- + Cr(CO)_6 \xrightarrow{n=1-4} Cr(CO)_6OH^- \quad (2)$$

$$Mo(CO)_{3,4}OH^- \xleftarrow{n=0} HO(H_2O)_n^- + Mo(CO)_6 \xrightarrow{n=1-4} Mo(CO)_6OH^- \quad (3)$$

$$W(CO)_{3,4}OH^- \xleftarrow{n=0} HO(H_2O)_n^- + W(CO)_6 \xrightarrow{n=1-4} W(CO)_6OH^- \quad (4)$$

examples of solvent-induced mechanism changes in gas-phase proton-transfer and substitution reactions have been reported.[8-10] In the present case, the observed maintenance of high reaction rates with even up to *four* solvent water molecules *without* solvent retention by the product ions must be a reflection of the strongly exothermic attachment of OH^- to the metal carbonyls.[11] Indeed, the observation of a fast reaction between $OH(H_2O)_4^-$ and $Fe(CO)_5$ permits an estimate of a lower limit to $D°[Fe(CO)_5\text{–}OH^-]$ of ≥ 50 kcal/mol.[12]

Several gas-phase ion–molecule reactions of $Fe(CO)_5OH^-$ have been observed in the flowing afterglow that support a structural formulation as the iron carboxylic acid **1**. Fe(C-

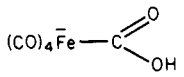

1

$O)_5OH^-$ is not observed to undergo binary neutral switching type reactions with molecules possessing large permanent dipole moments (i.e., CH_3NO_2, $\mu_D = 3.86$ D)[13] such as might be expected if it were an electrostatically bound cluster ion, $[Fe(CO)_5\cdots OH^-]$.[11,14] Furthermore, $Fe(CO)_5OH^-$ and its deuterated analogue,[5] $Fe(CO)_5OD^-$, both undergo hydrogen–deuterium exchange in the presence of carboxylic acids and H_2S (eq 5–7). We take this observation as evidence against an isomeric formate structure, $[Fe(CO)_4O_2CH]^-$, since exchange of a formyl hydrogen under these conditions is unlikely.

$$(CO)_4FeCOOD^- + HCO_2H \rightarrow (CO)_4FeCOOH^- + HCO_2D \quad (5)$$

$$(CO)_4FeCOOH^- + CH_3CO_2D \rightarrow (CO)_4FeCOOD^- + CH_3CO_2H \quad (6)$$

$$(CO)_4FeCOOD^- + H_2S \rightarrow (CO)_4FeCOOH^- + HSD \quad (7)$$

We therefore assign the iron carboxylic acid structure, **1**, to $Fe(CO)_5OH^-$ and, by analogy, we presume the other metal carbonyl/OH^- adducts in eq 2–4 to be anionic metallocarboxylic acids. Their occurrence as relatively stable gas-phase species has an important bearing on the continuing efforts to determine the mechanisms by which certain metal carbonyls may catalyze the water gas shift reaction in alkaline solution.[1-3] In particular, although $Fe(CO)_4COOH^-$ has been postulated as a key intermediate in WGSR catalysis by $Fe(CO)_5$,[15-17] it has never been observed directly and the exact

(1) Ford, P. C., Ed. "Catalytic Activation of Carbon Monoxide"; American Chemical Society: Washington, DC, 1981; ACS Symp. Ser. No. 152.
(2) King, R. B., Ed. "Inorganic Compounds with Unusual Properties"; American Chemical Society: Washington, DC, 1979; Adv. Chem. Ser. No. 173.
(3) Darensbourg, D. J.; Rokicki, A. *Organometallics* **1982**, *1*, 1685–1693 and references cited therein.
(4) All experiments were carried out in our recently constructed flowing afterglow apparatus which consists of a 100 cm × 7.6 cm i.d. ion-flow reactor with a quadrupole mass spectrometer detector (P(He) = 0.300 torr, $\bar{v}$ = 9100 cm s^{-1}, T = 300 ± 2 K). For general discussions of flowing afterglow, see: Ferguson, E. E.; Fehsenfeld, F. C.; Schmeltekopf, A. *Adv. At. Mol. Phys.* **1969**, *5*, 1–56. Smith, D.; Adams, N. G. In "Gas Phase Ion Chemistry"; Bowers, M. T., Ed.; Academic Press: New York, **1979**; Chapter 1.
(5) Most of the studies reported here have actually employed $DO(D_2O)_n^-$ reactant ions in order to avoid potential ambiguities arising from the equal mass-to-charge ratios for $^{35}Cl^-$ and $HO(H_2O)^-$.
(6) Measured bimolecular rate coefficients (in units of 10^{-9} cm^3 molecule^{-1} s^{-1}): 2.3 (n = 0); 2.3 (n = 1); 2.1 (n = 2); 1.8 (n = 3); 0.97 (n = 4).
(7) Similar reactions with $Fe(CO)_5$ and other mononuclear metal carbonyls are observed for a variety of gas-phase anions: Lane, K. R.; Sallans, L.; Squires, R. R., manuscript in preparation. For an earlier report on reactions between gaseous anions and $Fe(CO)_5$ see: Foster, M. S.; Beauchamp, J. L. *J. Am. Chem. Soc.* **1975**, *97*, 4808–4814.
(8) Bohme, D. K.; Rakshit, A. B.; Mackay, G. I. *J. Am. Chem. Soc.* **1982**, *104*, 1100–1101 and references cited therein.
(9) Bartmess, J. E. *J. Am. Chem. Soc.* **1980**, *102*, 2483–2484.
(10) Caldwell, G.; Rozeboom, M. D.; Kiplinger, J. P.; Bartmess, J. E. *J. Am. Chem. Soc.* **1984**, *106*, 809–810.
(11) Bohme, D. K. In "Ionic Processes in the Gas Phase"; Ferreira, M. A. A., Ed.; D. Reidel Publishing Co.: Dordrecht, 1984.
(12) Based upon data from: Payzant, J. D.; Yamdagni, R.; Kebarle, P. *Can. J. Chem.* **1971**, *49*, 3308–3314. Arshadi, M.; Kebarle, P. *J. Phys. Chem.* **1970**, *74*, 1483–1485. ($D°[4(H_2O)\text{–}OH^-]$ = 72.2 kcal/mol; estimated entropy contribution of 73.9 eu for reaction 1 (n = 4).)
(13) McClellan, A. L. "Table of Experimental Dipole Moments"; Rahara Enterprises: El Cerrito, CA, 1979; Vol. 2.
(14) Fahey, D. W.; Bohringer, H.; Fehsenfeld, F. C.; Ferguson, E. E. *J. Chem. Phys.* **1982**, *76*, 1799–1805.

0020-1669/84/1323-1999$01.50/0